Available online at www.sciencedirect.com
ScienceDirect
Trans. Nonferrous Met. Soc. China 20(2010) 537−546
Transactions of Nonferrous Metals Society of China
www.tnmsc.cn

Fretting wear of micro-arc oxidation coating prepared on Ti6Al4V alloy

LIN Xiu-zhou(林修洲)[1, 2], ZHU Min-hao(朱旻昊)[1], ZHENG Jian-feng(郑健峰)[1],
LUO Jun(罗　军)[1], MO Ji-liang(莫继良)[1]

1. Tribology Research Institute, Traction Power State Key Laboratory, Southwest Jiaotong University, Chengdu 610031, China;
2. Sichuan Province Key Laboratory for Corrosion and Protection of Materials, Sichuan University of Science and Engineering, Zigong 643000, China

Received 2 March 2009; accepted 4 May 2009

Abstract: Micro-arc oxidation (MAO) coating was prepared on Ti6Al4V alloy surface and its characterizations were detected by Vickers hardness tester, profilometer, scanning electric microscope (SEM), energy dispersive X-ray spectrometer (EDX) and X-ray diffractometer (XRD). Fretting wear behaviors of the coating and its substrate were comparatively tested without lubrication under varied displacement amplitudes (*D*) in a range of 3−40 μm, constant normal load (F_n) of 300 N and frequency of 5 Hz. The results showed that the MAO coating, presenting rough and porous surface and high hardness, mainly consisted of rutile and anatase TiO_2 phases. Compared with the substrate, the MAO coating could shift the mixed fretting regime (MFR) and slip regime (SR) to a direction of smaller displacement amplitude. In the partial slip regime (PSR), lower friction coefficients and slight damage appeared due to the coordination of elastic deformation of contact zones. In the MFR, the friction coefficient of the coating was lower than that of the substrate as a result of the prevention of plastic deformation by the hard ceramic surface. With the increase of the displacement amplitude, the degradation of the MAO coating and the substrate increased extremely. The fretting wear mechanisms of the coating were abrasive wear and delamination with some material transfer of specimen. In addition, the coating presented a better property for alleviating fretting wear.

Key words: titanium alloy; micro-arc oxidation; friction and wear; fretting wear

1 Introduction

Titanium alloys have been widely applied in aviation industry, exploitation of ocean, artificial implants of human body and so on, for their excellent properties, such as high melting point, high corrosion resistance, high specific strength rate and bioactivity [1−2]. However, they are seriously limited in some applications for low rigidity and wear resistance. Therefore, various surface modifying techniques such as salt cyaniding[3], laser treatment[4], PVD TiN coating[4], nitriding[5] and plasma immersion ion implantation (PIII) treatment[6], were introduced in order to improve their performances in the practical applications. Recently, a new surface modifying technique conventionally called micro-arc oxidation (MAO) which is characterized by high productivity, economic efficiency, ecological friendliness, high hardness, good wear resistance and excellent bonding strength with the substrate, is attracting increasing interest[7−9]. Micro-arc oxidation is an electrochemical surface modifying technique that would form ceramic-like coating on the surface of some non-ferrous metals (such as aluminum, magnesium, titanium and their alloys) by spark/arc micro-discharges[10−12].

In recent years, the tribological properties of the MAO coatings prepared on the surface of titanium alloys have been studied by some scholars under dry and solid lubrication sliding condition[13−15]. However, almost all researches focused on the conditions of reciprocating and pin-on-disk sliding and discussions of the friction coefficients and wear loss.

It is well known that fretting is caused by the relatively oscillatory movement of small amplitude, which may lead to service failure due to rapid crack

Foundation item: Project(50521503) supported by the National Natural Science Foundation of China; Project(2007CB714704) supported by the National Basic Research Program of China; Project(200536) supported by the Foundation of the Author of National Excellent Doctoral Dissertation of China
Corresponding author: ZHU Min-hao; Tel +86-28-87600715; Fax: +86-28-87601342; E-mail: zhuminhao@swjtu.cn
DOI: 10.1016/S1003-6326(09)60175-8

formation and surface wear[16−17]. In fact, many industrial applications of titanium alloys are operated under fretting conditions; however, few reports on the fretting behaviors of the MAO coating can be indexed up to the present[18]. In the pervious work[19], the characterization and wear mechanism of the MAO coating prepared on LD11 aluminium alloy under the condition of fretting wear have been studied in detail. It was shown that the MAO coating shifted the mixed fretting regime and slip regime to the direction of smaller displacement and presented better property of anti-fretting wear. Therefore, the fretting behaviors of the MAO coating prepared on Ti6Al4V titanium alloy were studied to understand its running behaviors and damage mechanisms under fretting wear conditions.

2 Experimental

2.1 Preparation and characterization of coating

Ti6Al4V (6.020% Al, 4.100% V, 0.168% Fe, 0.160% O, 0.043% C and balance Ti, mass fraction) was used as the substrate material, which was machined to a size of 8 mm×8 mm×20 mm and then polished to a surface roughness R_a of approximately 0.050 μm. Prior to coating deposition, the specimens were ultrasonically cleaned in the acetone and thoroughly dried in air.

The MAO coating was deposited by a self-manufactured micro-arc oxidation device with the maximum power of 60 kW (Fig.1). The electrolyte mainly consisted of sodium phosphate, sodium silicate and some additives. During the coating deposition, the electrolyte temperature was controlled below 40 ℃ by using magnetic stirrer and circle-cooling water system. The MAO coating with well surface quality and thickness of 10 μm could be deposited through adjusting the amount of additives, electric current intensity and voltage.

The surface roughness and micro-hardness of the coating and substrate were measured by using Ambios XP-2 profilometer and Akashi MVK-H21 Vickers hardness tester, respectively. The chemical compositions and phase structures of the coating were analyzed by energy dispersive X-ray spectrometer (EDX, EDAX-7760/68 ME) and X-ray diffractometer (XRD, Phlips X’Pert PRO). The morphologies of the coating surface were evaluated by scanning electron microscopy (SEM, Qunta2000).

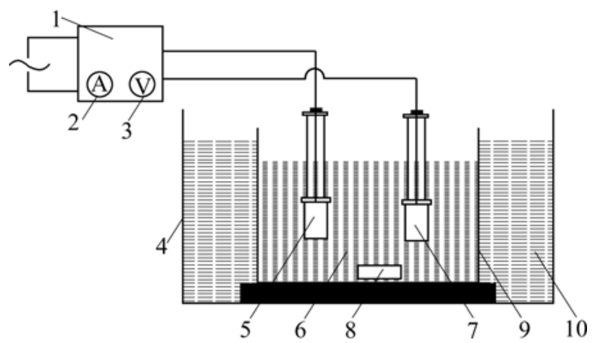

Fig.1 Scheme of micro-arc oxidation device: 1—DC power supply; 2—Current meter; 3—Voltage meter; 4—Container; 5—Specimens; 6—Electrolyte; 7—Cathode; 8—Magnetic muddler; 9—Electrolytic tank; 10—Cooling water

2.2 Fretting wear tests

A hydraulic fretting wear test rig, as shown in Fig.2, was used to test the fretting wear behaviors of the MAO coating and the substrate under a ball-on-flat contact configuration. The ball specimen was fixed at the holder and reciprocatingly moved with the piston of the hydraulic system. The flat specimen was fixed on the holder, which was connected with a lord sensor to measure friction force. The relative displacement of the contact pairs was measured by the displacement sensor. The normal load (F_n) between the pairs was applied by a loading system, which mainly consists of spring and screw. During the fretting test, the whole fretting process was computerized and the variations of displacement and normal load can be realtimely and automaticly recorded as a function of cycles.

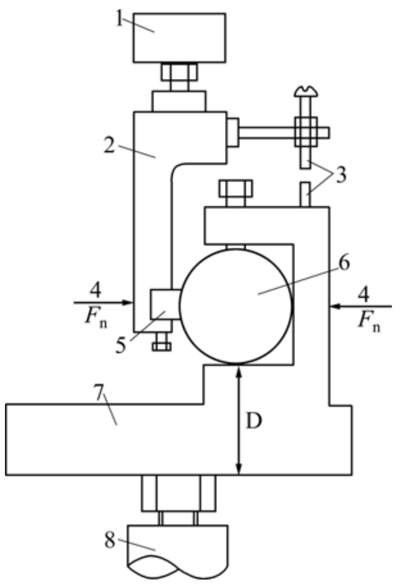

Fig.2 Schematic diagram of fretting wear test rig: 1— Load sensor (measuring friction force); 2—Holder of flat specimen; 3—Applied displacement sensor; 4—Loading system of normal load; 5—Flat specimen; 6—Ball specimen; 7—Holder of ball specimen; 8— Piston of hydraulic system

A GCr15 steel ball with a diameter of 40 mm, surface roughness R_a of 0.030 μm and hardness of HRC 61−65, was used as the spheric specimen. All fretting wear tests were performed in ambient atmospheric condition ((23±1) ℃ and (40±5)% relative humidity) without lubrication; the displacement amplitudes (D)

varied in the range of 3−40 μm; the normal load (F_n) was imposed at 300 N; the frequency was set at 5 Hz; and the number of cycles varied from 1 to 10^4. After fretting wear tests, the morphologies of the fretting scars were examined by scanning electron microscope (SEM, QUANTA2000) and optical microscope (OM, OLYMPUS BX60MF5); the chemical compositions of the worn surface and debris were analyzed by energy dispersive X-ray spectrometer (EDX, EDAX-7760/68 ME) and the wear volume of fretting scars was measured by laser confocal scanning microscope (LCSM, OLYMPUS OLS1100).

3 Results and discussion

3.1 Coating characterizations

After micro-arc oxidation process, the surface Vickers hardness and surface roughness (R_a) of the specimens increased from $HV_{0.05}$ (323±16) and (0.037±0.008) μm to $HV_{0.05}$ (712±58) and (0.466±0.045) μm, respectively. The surface of MAO coating presented a typical porous ceramic structure with many crater-like cavities (see Fig.3). As indicated by the EDX spectra shown in Fig.4, compared with Ti6Al4V substrate, some additional elements (such as O, Si and P) were detected on the surface of the MAO coating, in which Si and P elements came from the solution, and O probably presented in TiO_2 and some in Al_2O_3 which generated during the micro-arc oxidation process. It was further verified by XRD analysis (as seen in Fig.5) that the MAO coating mainly consisted of anatase TiO_2 and rutile TiO_2, which were the primary contributions for the high hardness of coating, besides, a few phase of Ti and Al_2O_3 were found.

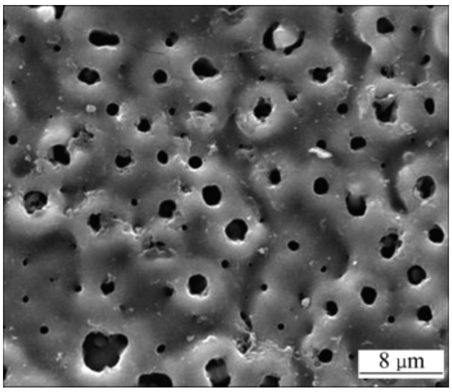

Fig.3 SEM micrograph of MAO coating

3.2 Fretting regimes

For comparison, fretting wear tests of the MAO coating and Ti6Al4V substrate against GCr15 steel balls were carried out under the same test parameters. According to the theory of fretting maps[20], three fretting regimes, i.e. partial slip regime (PSR), mixed

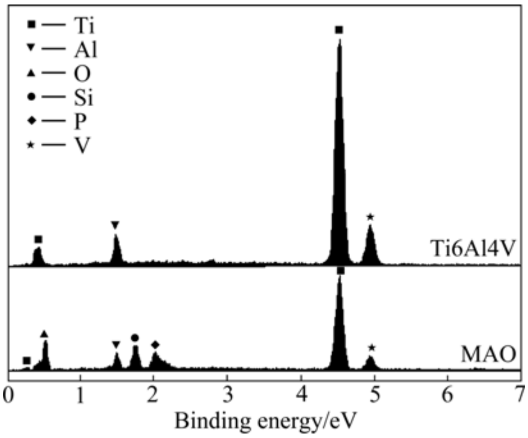

Fig.4 EDX spectra of Ti6Al4V substrate and MAO coating

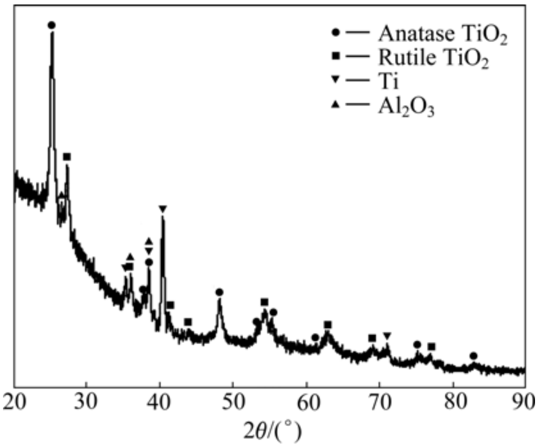

Fig.5 XRD patterns of MAO coating

fretting regime (MFR) and slip regime (SR), could be determined for both the coating and substrate by their fretting logs (F_t (tangential friction force) — D (displacement amplitude)—N (number of cycles) curves, see Fig.6).

Under a normal load of 300 N, at lower displacement amplitudes (less than 5 μm for the substrate alloy and less than 3 μm for the coating), F_t—D curves were all presented in shape of a line in all cycles. Thus, fretting ran in the regime of PSR. While for higher displacement amplitudes (more than 15 μm for the substrate alloy and more than 10 μm for the coating), all the F_t—D curves were open as parallelogram, indicating that the relative motions of gross slip took place during the entire fretting cycles[17, 20], i.e. the fretting ran in the SR. For Ti6Al4V alloy, the F_t—D curves appeared in shape of parallelogram at initial cycles (Fig.7(a)) when D=10 μm, corresponding to the fretting running in condition of gross slip, then the F_t — D curves transformed from parallelogram to elliptic shape at about 100 cycles (Fig.7(a)) while the relative motion transformed to partial slip. At last, the F_t—D curves gradually changed from elliptic to parallelogram loops after 10^3 cycles (Fig.7(a)). It was indicated that the fretting run in MFR was due to the vibration of relative motions between partial slip and gross slip[19]. For the MAO coating, the relative motions of gross slip at initial cycles transformed to partial slip after 100 cycles when D=5 μm (Fig.7(b)). Thus, the fretting running regime of the coating was also in MFR. Table 1 lists the fretting regime distributions of the MAO coating and its substrate. It can be observed that MFR and SR of the coating shifted to the direction of lower displacement amplitude as compared with those of the substrate. In other words, the relative slip easily occurred in the contact interfaces of MAO coating, which maybe attributed to a higher hardness of the MAO coating. The higher hardness of the coating caused the contact area to decrease corresponding to the increase of tangential stiffness, and thus induced a fretting regime transition at relatively low displacement amplitude.

A special phenomenon appeared in Fig.7 that the variation of the F_t—D curves as function of the number of fretting cycles were visibly different for the MAO coating and its substrate in the MFR. Both for the substrate and the MAO coating, the F_t—D curves presented initially in the shape of parallelogram and then changed to elliptical loops. Obviously, the area of the

Table 1 Distribution of fretting regimes under different displacement amplitudes

Displacement amplitude, D/μm	Ti6Al4V	MAO coating
3	PSR	PSR
5	PSR	MFR
10	MFR	SR
15	SR	SR
20	SR	SR
30	SR	SR
40	SR	SR

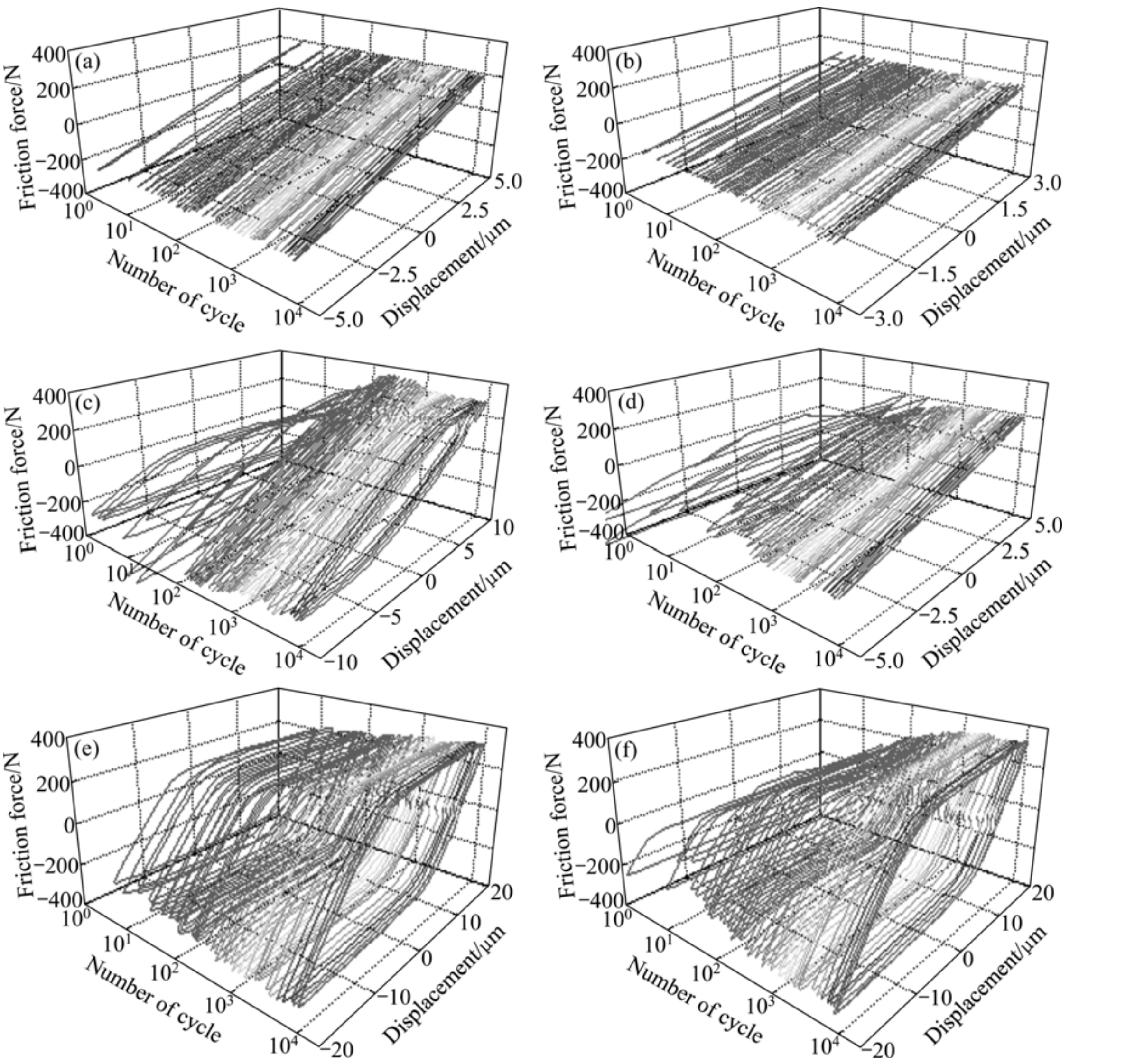

Fig.6 Fretting logs of MAO coating and Ti6Al4V alloy under different displacement amplitudes: (a) Ti6Al4V, D=5 μm; (b) MAO, D=3 μm; (c) Ti6Al4V, D=10 μm; (d) MAO, D=5 μm; (e) Ti6Al4V, D=20 μm; (f) MAO, D=20 μm

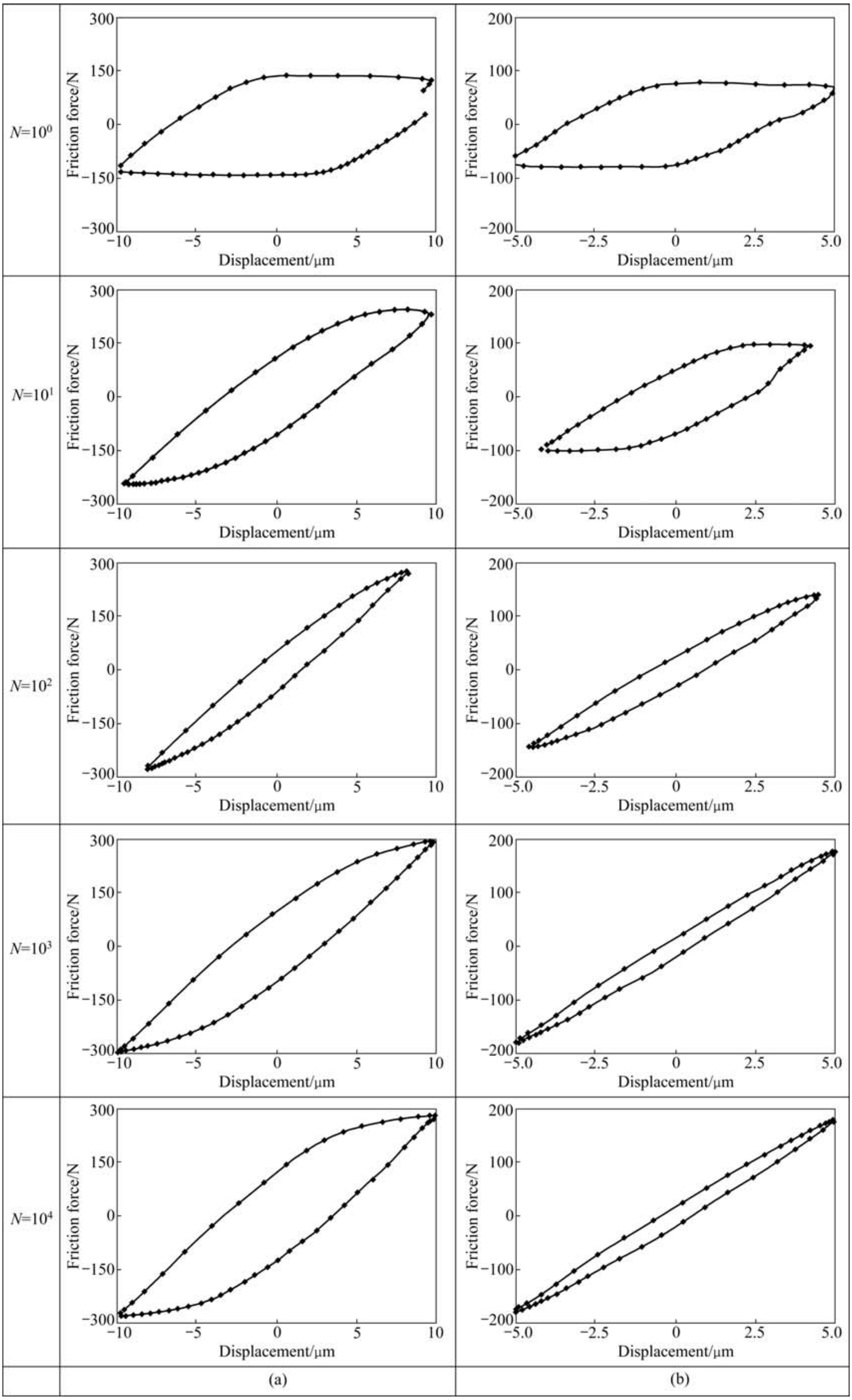

Fig.7 F_t—D curves of Ti6Al4V alloy and MAO coating at different numbers of cycle in mixed regime: (a) Ti6Al4V, D=10 μm; (b) MAO coating, D=5 μm

elliptic F_t—D curves for the substrate varied with the variation of the number of cycles, and the minimum area of the elliptic loop appeared at about 100 cycles (Fig.7(a)). However, for the coating, the area of the loops reduced gradually and monotonically with the increase of the number of cycles (Fig.7(b)). This implied that different interface behaviors occurred between the two kinds of contact counter-pairs. The "U" type variation of the area of F_t—D curves for the titanium alloy may be induced by the plastic deformation, work-hardening and detachment of particles. In other words, with the increase of the fretting cycles, the plastic deformation and work-hardening occurred successively, then the area of the F_t—D curve reached the minimal value when the accumulation of the work-hardening reached a very high level. Following this, the particles detached from the contact zone due to the high level work-hardening and induced the new undeformed titanium alloy exposed and taken part in the succeeding fretting cycles, which was corresponding to the wider elliptic loops. Differently, for the MAO coating, the hard ceramic layer on the surface inhibited the cyclic work-hardening occurred between the contact interfaces.

3.3 Coefficients of friction

As shown in Fig.8, the coefficients of friction (COF) for the MAO coating and the substrate presented three stages approximately: initial stage, ascent stage and stable stage. In initial stage, the coating presented lower COF and longer duration than that of the substrate since the hard surface of the coating could enhance the relative slip between the two contact surfaces and thus reduced the surface shear resistances. Also in Fig.8, it can be found that the COFs were quite different in the different fretting running regimes. In PSR, similar stable stage values of the COF at lower level exhibited both for the coating and the substrate due to the relative motion of the partial slip coordinated caused by elastic deformation. In MFR, main difference occurred in the ascent stage. High plastic deformation of titanium alloy resulted in a great rise of the COF; however, the coating retarded the plastic deformation of the substrate alloy and consequently reduced the COF greatly. In SR, with the increase of the displacement amplitude, the tangential forces of contact surfaces increased and the damage of the coating increased accordingly. Therefore, the stable value of COF approached that of the substrate after about 10^3 cycles.

3.4 Damage analyses

As mentioned above, the fretting running behaviors varied in different regimes. The damage morphologies and wear mechanisms are discussed according to the three regimes, respectively.

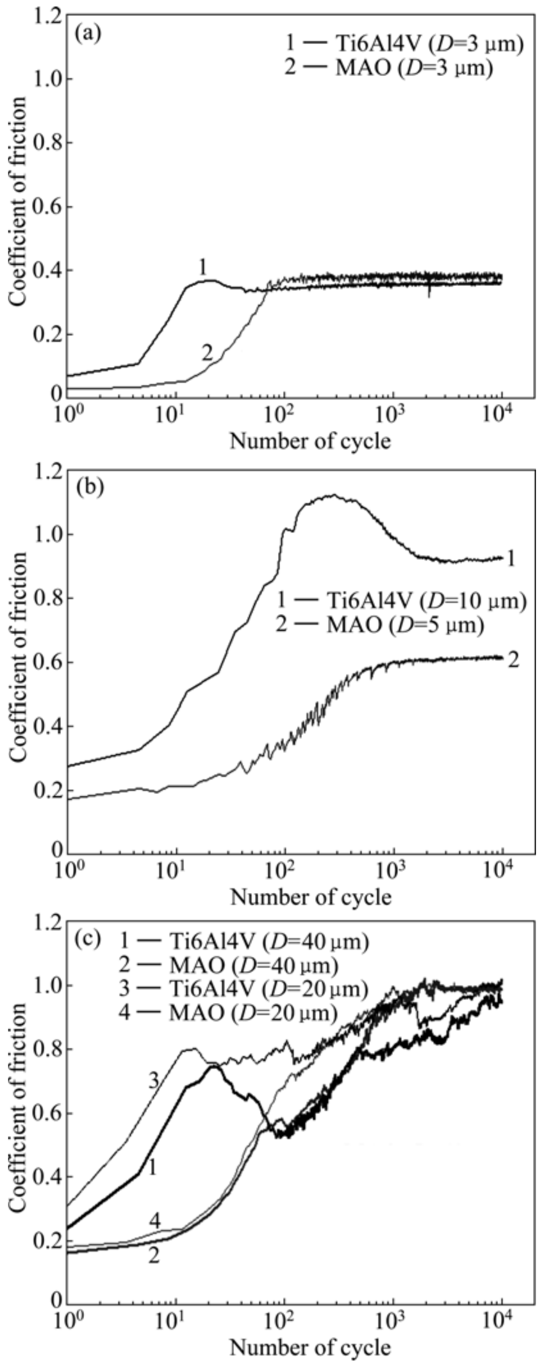

Fig.8 Friction coefficients of MAO coating and Ti-6Al-4V alloy in different fretting regimes: (a) Partial slip regime; (b) Mixed fretting regime; (c) Slip regime

3.4.1 In partial slip regime (PSR)

Fig.9 shows the morphologies of the fretting scars of the MAO coating and Ti6Al4V alloy in the PSR, which corresponded to the displacement amplitude of 3 μm. Relative motions in this regime were essentially accommodated by elastic deformation during the entire fretting processes, while the F_t—D curves were almost all closed. In this regime, according to the Mindlin's theory, no relative sliding takes place at the contact interfaces. In other words, the micro-slip occurred at the edge of contact zone and the contact center maintained the state of sticking from beginning to end. This is the reason why the morphology of the wear scar for the titanium alloy in Fig.9(a) was in a typical shape of annularity. However, for the fretting scars of the MAO coating, this typical morphology of annularity disappeared in the PSR (Fig.9(b)), and the porous structure of the coating maintained (Fig.9(c)). This is probably because that the characteristic of easy-sliding was presented by the MAO coating. Obviously, the damage of the coating was slighter than that of the substrate from Fig.9.

3.4.2 In mixed fretting regime (MFR)

As shown in Fig.10(a), clear trace of the plastic deformation flow and severe detachment could be

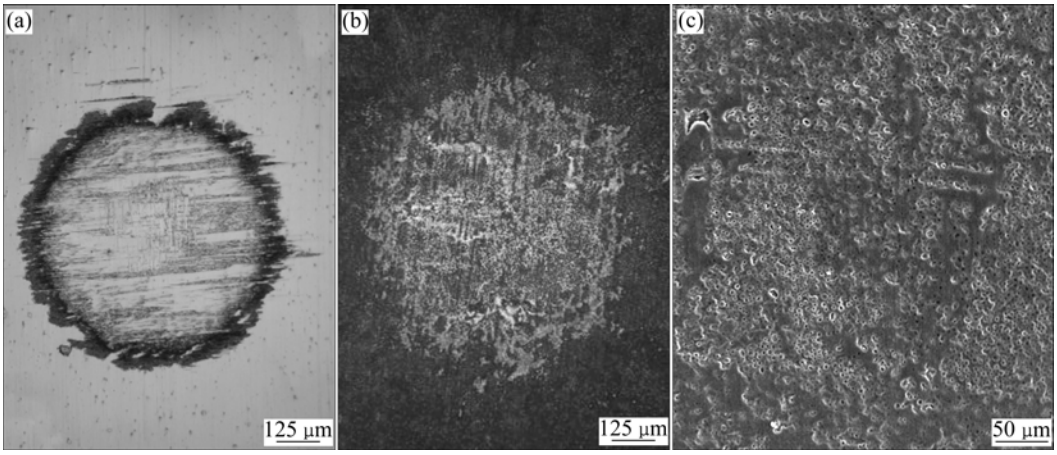

Fig.9 Morphologies of wear scar of MAO coating and Ti6Al4V alloy in partial slip regime: (a) Ti6Al4V (D=3 μm, OM); (b) MAO coating (D=3 μm, OM); (c) MAO coating (D=3 μm, SEM)

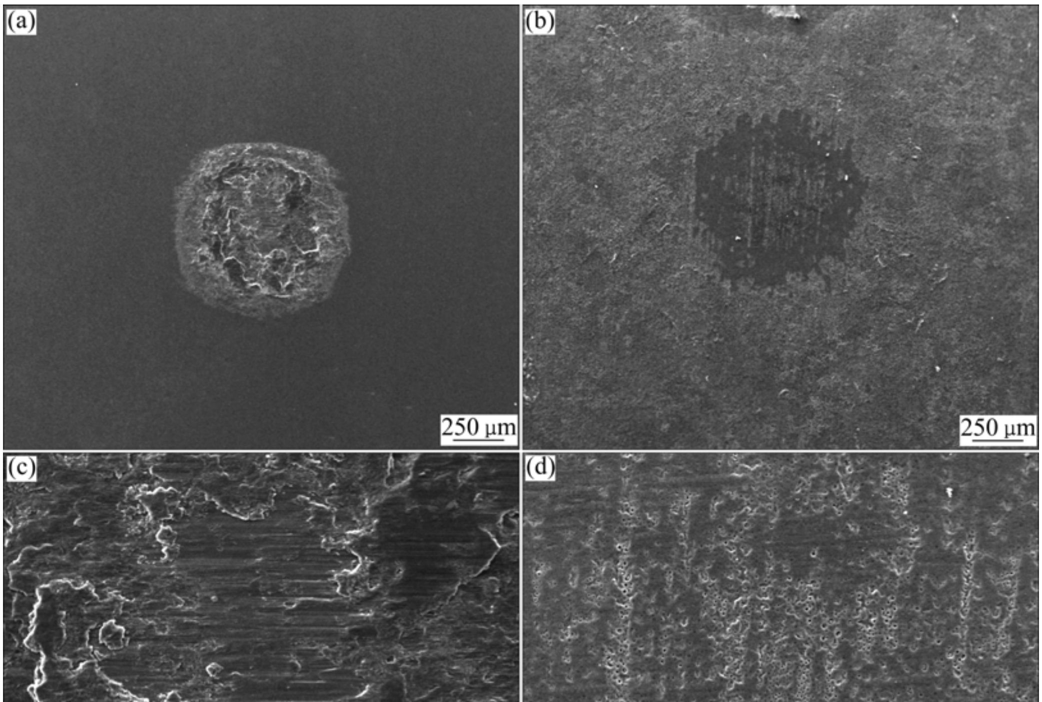

Fig.10 Morphologies of wear scar of MAO coating and Ti6Al4V alloy in mixed fretting regime: (a) and (c) Ti6Al4V (D=10 μm); (b) and (d) MAO coating (D=5 μm)

observed on the scar of the Ti6Al4V alloy, which induced the highest peak of the COF in the ascent stage in the MFR (Fig.8(b)). In addition, a third body contact formed due to some detached particles covering the contact zone. Ploughing traces for the typical morphology of abrasive wear were observed on the fretting scars of the substrate specimens (Fig.10(c)).

For the coating, the wear was aggravated slightly from the PSR to the MFR with the increase of displacement amplitude. However, by comparing Fig.10(a) with Fig.10(b), it is found that the damage of the coating was slighter than that of the substrate. Two portions could be observed in Fig.10(b), which was probably induced by the different fretting running steps. The inner wear zone (i.e. the contact center) presented apparent sliding vestige due to gross slip occurred at early 100 cycles (Fig.7(b)). And the lateral portion of the scar was formed mainly owing to the partial slip, which was corresponding to the elliptic F_t—D curves. The pore-rich structure of the coating could still be observed on the contact zone in the MFR (Fig.10(d)). Iron element was detected by the EDX (Fig.11). It is the result that the material transferred from the ball specimen, which implys the MAO coating exposed a better wear resistance due to its high hardness. The MFR was proved

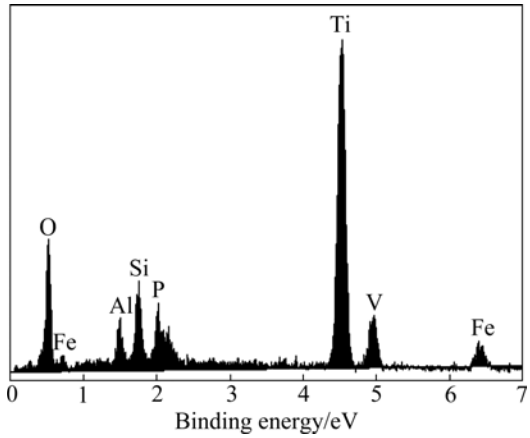

Fig.11 EDX spectrum of center area of wear scar of MAO coating in mixed fretting regime

to be the most dangerous regime for crack nucleation and service failure[20]. However, the protection effect for this coating maintained after 10^4 cycles, which helped to alleviate fretting damage.

3.4.3 In slip regime(SR)

When the displacement amplitudes were higher, the fretting regime entered into the SR and the degradation of Ti6Al4V alloy increased greatly (see Fig.12(a)). As

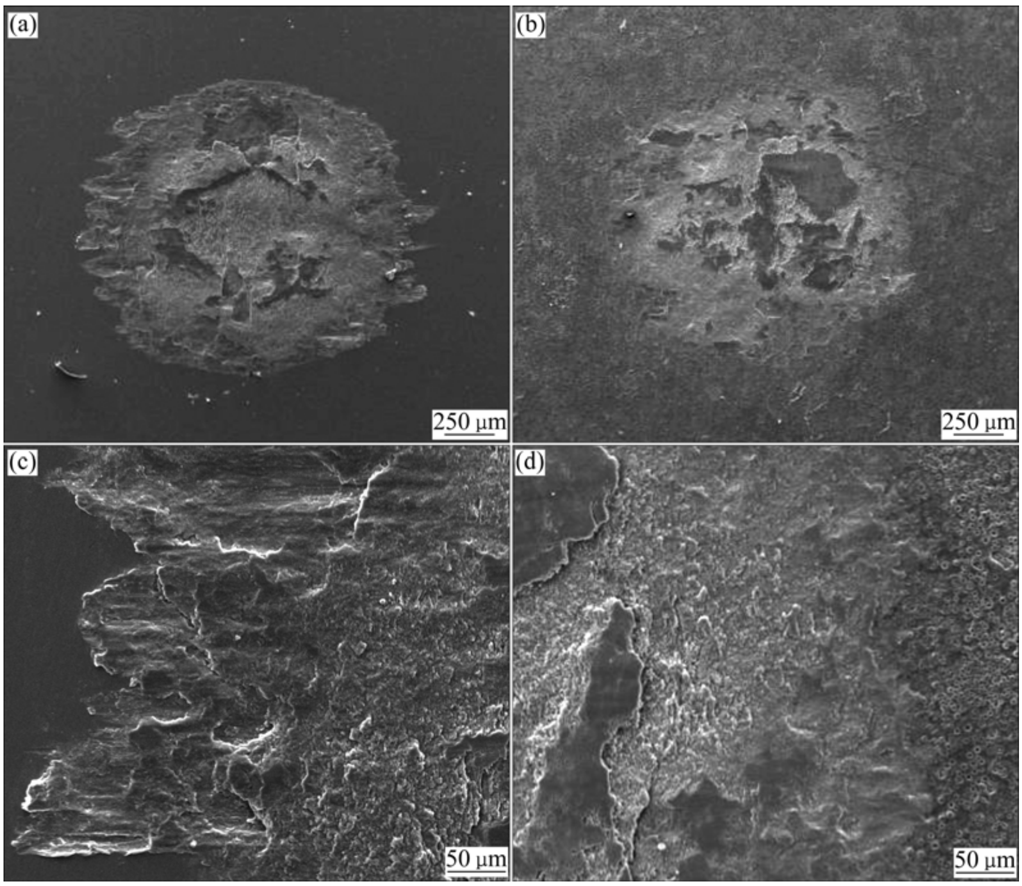

Fig.12 Morphologies of wear scar of MAO coating and Ti6Al4V alloy in slip regime: (a) and (c) Ti6Al4V (D=40 μm); (b) and (d) MAO coating (D=40 μm)

shown in Figs.12(a) and (c), particles detached by delamination, ploughing traces and debris accumulation appeared obviously on the wear scar. A thicker wear debris layers covered the contact centre and the detachment marks distributed at the edge area of the scars with a dissimilar morphology in different sections. High oxygen peaks were detected by the EDX on the scars of the titanium alloy specimens in the SR. Therefore, for the substrate alloy, the fretting wear mechanisms were mainly abrasive wear, oxidative wear and delamination.

For the coating, in the SR, with the increase of the displacement amplitudes, the degradation increased also but was evidently slighter than that of the substrate specimens under the same test conditions. As shown in Figs.12(b) and (d), to compare with the substrate, similar damage morphologies were obtained for the coating. The abrasive wear and delamination were still the wear mechanisms for the coating. In addition, also similar to the MFR, it was found that the material transferred from the ball specimen. More materials of the ball specimen were removed than those of the titanium alloy against steel ball, which indicated that the coating presented a better resistance of fretting wear. As seen in Figs.12(b) and (d), some dark zones on the scars were the coating which was undetached. Therefore, even after 10^4 cycles, the protection effect of the coating still existed partially although the COF has reached the value of the substrate material.

Fig.13 shows the results of wear volumes for the MAO coating and the substrate specimen by using the LCSM. It is indicated that the wear volume of the coating was extremely lower than that of the substrate under the same test condition. In addition, the effect of alleviating fretting wear for the coating was increased greatly with the increase of the displacement amplitude. In sum, the fretting wear resistance of Ti6Al4V alloy was enhanced greatly by the micro-arc oxidation technology.

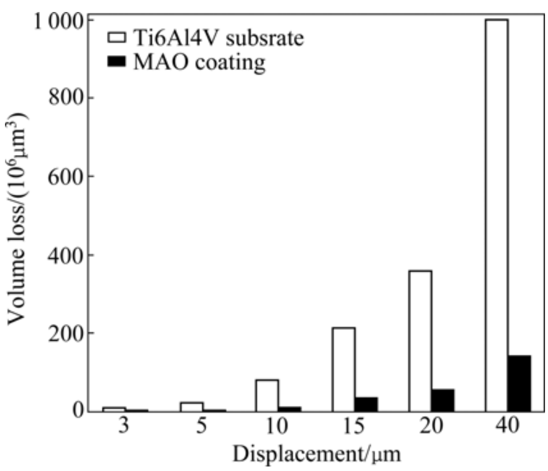

Fig.13 Wear volumes of MAO coating and Ti6Al4V alloy under varied displacement amplitudes

4 Conclusions

1) The MAO coating with rough surface, typical crater-like pore-rich ceramic structure and high hardness was obtained, which mainly consisted of phases of rutile, anatase TiO_2 and a little Al_2O_3.

2) Three fretting running regimes (PSR, MFR and SR) were determined by the evolutions of the F_t—D curves for both the MAO coating and Ti6Al4V alloy substrate. The MAO coating could shift the MFR and SR to the direction of smaller displacement amplitude, and presents characteristics of easy sliding.

3) Both for the Ti6Al4V substrate and the MAO coating, three stages of friction coefficients were found. Lower COF exhibited in the initial stage; and the duration of initial and ascent stages reduced with the increase of the displacement amplitude. In the PSR, lower friction coefficients appeared due to the coordination of elastic deformation of the contact zones. In the MFR, the friction coefficients of the coating were lower than those of the substrate since the hard ceramic layer avoided the plastic deformation of the substrate alloy. Similar stable values of COF in the SR appeared for the coating and the titanium alloy.

4) The fretting wear mechanisms for the coating were abrasive wear and delamination with some material transfer of ball specimen. However, for the substrate alloy, oxidative wear was also one of wear mechanisms. The measurement of wear volumes showed that the coating presented a better property for alleviating fretting wear.

References

[1] ZHOU Lian, LUO Guo-zhen. Research and development of titanium in China [J]. Materials Science and Engineering A, 1998, 243: 294−298.

[2] SCHUTZ R W, SATKIN H B. Recent developments in titanium alloy application in the energy industry [J]. Materials Science and Engineering A, 1998, 243: 305−315.

[3] LAI F D, WU T I, WU J K. Surface modification of Ti-6Al-4V alloy by salt cyaniding and nitriding [J]. Surface and Coating Technology, 1993, 58: 79−81.

[4] YILBAS B S, SHUJA S Z. Laser treatment and PVD TiN coating of Ti-6Al-4V alloy [J]. Surface and Coating Technology, 2000, 130: 152−157.

[5] ZHECHEVA A, SHA W, MALINOY S, LONG A. Enhancing the microstructure and properties of titanium alloys through nitriding and other surface engineering methods [J]. Surface and Coating Technology, 2005, 200(7): 2192−2207.

[6] MANDL S. PIII treatment of Ti alloys and NiTi for medical applications [J]. Surface and Coating Technology, 2007, 201(15): 6833−6838.

[7] YEROKHIN A L, NIE X, LEYLAND A, MATTHEWS A. Characterisation of oxide films produced by plasma electrolytic oxidation of a Ti-6Al-4V alloy [J]. Surface and Coating Technology, 2000, 130: 195−206.

[8] XUE Wen-bin, WANG Chao, CHEN Ru-yi, DENG Zhi-wei. Structure and properties characterization of ceramic coatings produced on Ti-6Al-4V alloy by microarc oxidation in aluminate solution [J]. Materials Letters, 2002, 52: 435−441.

[9] GUO H F, AN M Z, HUO H B, XU S, WU L J. Microstructure characteristic of ceramic coating fabricated on magnesium alloys by micro-arc oxidation in alkaline silicate solutions [J]. Applied Surface Science, 2006, 252(22): 7911−7916.

[10] XUE Wen-bin, DENG Zhi-wei, CHEN Ru-yi, ZHANG Tong-he. Growth regularity of ceramic coating formed by microarc oxidation on Al-Cu-Mg alloy [J]. Thin Solid Films, 2000, 372: 114−117.

[11] YAO Zhong-ping, JIANG Yan-li, JIANG Zhao-hua, WANG Fu-ping, WU Zhen-dong. Preparation and structure of ceramic coatings containing zirconium oxide on Ti alloy by plasma electrolytic oxidation [J]. Journal of Materials Processing Technology, 2008, 205: 303−307.

[12] PENG Ji-hua, LI Wen-fang, HAN Bing, HUANG Fang-liang, DU Jun. Synthesis of tetragonal $BaTiO_3$ film on Ti substrate by micro-arc oxidation [J]. Transactions of Nonferrous Metals Society of China, 2008, 18: 1117−1121.

[13] KRISHNA L R, SOMARAJU K R C, SUNDARAJAN G. The tribological performance of ultra-hard ceramic composite coating obtained through microarc oxidation [J]. Surface and Coating Technology, 2003, 163/164: 484−490.

[14] WANG Y M, LEI T Q, JIA D C, ZHOU Y, OUYANG J H. Tribological behavior of microarc oxidation coatings formed on titanium alloys against steel in dry and solid lubrication sliding [J]. Applied Surface Science, 2006, 252(8): 2989−2998.

[15] SUN Xue-tong, LIN Cheng-xin. Tribological behaviour of ceramic coatings formed on titanium alloy through micro-arc oxidation technique [J]. Key Engineering Materials, 2007, 353/358: 898−901.

[16] WATERHOUSE R B. Fretting fatigue [M]. London: Applied Science, 1981.

[17] ZHOU Zhong-rong, VINCENT L. Cracking induced by fretting of aluminium alloys [J]. Journal of Tribology Transactions of the ASME, 1997, 119: 36−42.

[18] WANG Y M, LEI T Q, GUO L X, JIANG B L. Fretting wear behaviour of microarc oxidation coatings formed on titanium alloy against steel in unlubrication and oil lubrication [J]. Applied Surface Science, 2006, 252(23): 8113−8120.

[19] ZHU Min-hao, CAI Zhen-bing, LIN Xiu-zhou, REN Ping-di, TAN Juan, ZHOU Zhong-rong. Fretting wear behaviour of ceramic coating prepared by micro-arc oxidation on Al-Si alloy [J]. Wear, 2007, 263: 472−480.

[20] ZHOU Zhong-rong, VINCENT L. Mixed fretting regime [J]. Wear, 1995, 181/183: 531−536.

(Edited by FANG Jing-hua)